PIIb-01

2-Chlorobutane racemization process in DMF solution: Application of hybrid MC/MD reaction method

Yuichi Suzuki[1], Takuya Okamoto[1], Norio Takenaka[1,2] and Masataka Nagaoka[1,2]
[1]*Graduate School of Information Science, Nagoya University, Furo-cho, Chikusa-ku, Nagoya 464-8601, Japan*
[2]*ESICB, Kyouto University, Katsura, Nishikyou-ku, Kyoto 615-8510, Japan*
e-mail address: suzuki@ncube.nagoya-u.ac.jp

I. Introduction

In diffusion in solids and chemical reactions, etc, many dynamical systems spend the majority of their time in phase space regions, e.g. 99.9999999% in the initial state of N_2O_4 dissociation reaction at 273 K. With traditional molecular simulations, it is difficult to determine the stereochemical characteristics that originate in such rare events.

II. Method

We have developed the hybrid Monte Carlo (MC)/molecular dynamics (MD) reaction method with rare event-driving mechanism to treat such complex reacting systems and applied it to 2-chlorobutane racemization in DMF solution [1]. The present model system consists of 50 (*R*)-2-chlorobutane and 350 *N*,*N*-dimethylformamide (DMF) molecules (1.65 mol/L). The temperature was maintained at 313K by applying a weak coupling algorithm.

III. Results and Discussion

The changes of numbers of (*R*)- and (*S*)-2-chlorobutane molecules and 2-butyl cations are shown in Figure 1. The equilibrium numbers, estimated as averages over last 100 MC/MD cycles, were 25.3, 24.4 and 0.3, respectively. Thus, racemization could be realized satisfactorily within thermal fluctuation of the numbers of molecules. Figure 2 shows typical snapshots of 2-chlorobutane DMF solution in the initial (0 MC/MD cycle) (Figure 2a) and equilibrium state (897 MC/MD cycles) after racemization (Figure 2b). (*R*)- and (*S*)-2-chlorobutane are distributed homogeneously, together with other species, i.e., one 2-butyl cation, one chloride ion and 350 DMF molecules. In conclusion, the present method worked very well to realize a stereochemical mechanism for the racemization.

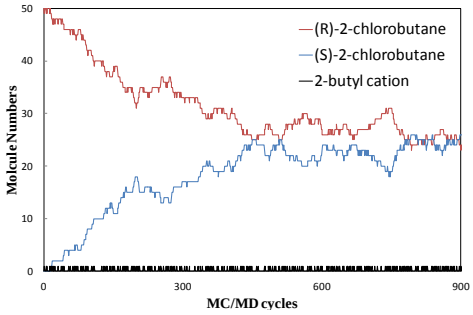

Fig.1 Number changes during the hybrid MC/MD reaction simulations.

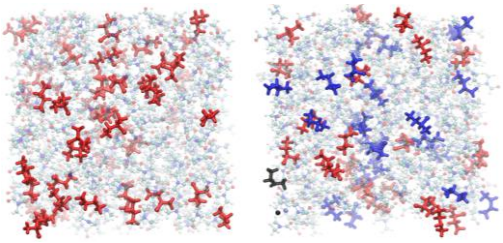

(a) Initial state (b) Equilibrium state

Fig.2 Snapshots of (a) the initial and (b) a typical equilibrium configuration consisting of (*R*)-(red), (*S*)-2-chlorobutane molecules (blue), a 2-butyl cation and a chloride ion (black).

[1] M. Nagaoka, Y. Suzuki, T. Okamoto, N. Takenaka, *Chem. Phys. Lett.*, **583**, 80 (2013).

PIIb-02

Ab Initio SemiClassical Molecular Dynamic (AI-SCMD) with ZN-TSH approach --- Photodissociation process for Hydrogen Sulfide

Tatsuhiro Murakami[1], Yoshiaki Teranishi[2], Alexey Kondorskiy[3], Hiroki Nakamura[4] and Shinkoh Nanbu[1]

[1]*Faculty of Science & Technology, Sophia Univ., 7-1 Kioi-cho, Chiyoda-ku, Tokyo 102-0094, Japan*
[2]*Inst. of Physics, National Chiao Tung Univ., 1001 Ta Hsueh Rd., Hshinchu, 30010, Taiwan*
[3]*P. N. Lebedev Physical Inst., Leninsky pr., 53, Moscow 119991 and Moscow Institute of Physics and Technology, Institutsky per., 9, Dolgoprudny, Moscow Region 141700, Russia*
[4]*Inst. of Molecular Science, National Chiao Tung Univ., 1001 Ta Hsueh Rd., Hshinchu, 30010, Taiwan*
e-mail address: tatsuh-m@sophia.ac.jp

Abstract

We proposed *Ab Initio* SemiClassical Molecular Dynamic (AI-SCMD) with ZN-TSH approach in this paper; our presentation shows how the result of on-the-fly nonadiabatic *ab initio* Molecular Dynamics (AI-MD) simulations could be utilized to obtain the phase-information caused by quantum effect in a molecular system which has many degrees of freedom. And also the parameters for hopping classical trajectories calculated by Zhu-Nakamura version of the trajectory surface hopping (ZN-TSH) method are used to perform the wavepacket propagation on the Herman-Kluk (HK) semiclassical frozen Gaussian propagation scheme. The demonstration of this new approach will be conducted performing full-dimensional AI-SCMD simulations of three photo-chemical processes like photodissociation dynamics of H_2S.

PIIb-03

Adsorption states of NO molecule on stepped and kinked Pt(111) surfaces studied by DFT simulations

Satoshi Makihara, Daisuke Mimura, Kouji Inagaki, Yoshitada Morikawa
Graduate School of Engineering, Osaka University
2-1 Yamada-oka, Suita, Osaka 565-0871, Japan
e-mail address: makihara@cp.prec.eng.osaka-u.ac.jp

I. Introduction

NO*x* reduction reaction is important catalytic reactions of the three-way-catalysts (TWC). Therefore the understanding of interaction of NO*x* with catalytic metal surfaces is of great importance to design more reactive catalysts with smaller amount of precious metals. As is well known, real catalytic surfaces have much more complicated structures than those of single-crystal clean surfaces and catalytic reactions on metal surfaces often take place at defect sites such as steps and kinks. Recently, Tsukahara et al. reported a metastable adsorption state of which NO, primary component of the NO*x*, stretching vibrational frequencies ν(N-O) is 1385cm^{-1} by IRAS [1] and tentatively assigned it to the stretching mode of NO adsorbed at a threefold hollow site on the lower terrace (lower fcc site) near the step site. However, by DFT calculation, ν(N-O) of this hollow site was calculated to be 1470 cm^{-1} [2], larger than the experimental value by more than 80 cm^{-1}. In this research, we investigated the adsorption states of NO at and near the Pt step and kink sites and search an adsorption state of which ν(N-O) is close to the experimental value of 1385cm^{-1}[1] by using DFT simulations.

Ⅱ. Results and discussion

Figure 1 shows most stable adsorption states at the Pt step and kink sites. We found Pt kinked site (Fig. 1(b)) is more stable than the Pt stepped and terrace sites. This result indicates the Pt kinked sites play a much more prominent role in NO reduction reaction on Pt catalytic surfaces. We also calculated ν(N-O) of many NO adsorption states including lower fcc site near the step and kink site. Our calculated values of ν(N-O) accord well with experimental values[1], but ν(N-O) of lower fcc site is much larger than experimental values (Table. 1). However, we found some new adsorption states near the Pt stepped and kinked sites, especially, one adsorption state with ν(N-O) close to 1385cm^{-1} near the Pt kinked site and the details will be described in the poster presentation.

Table 1. Adsorption energy E_{ad} and ν(N-O) .

System	Site	E_{ad} [eV]	ν(N-O) [cm^{-1}]	ν(N-O){exp.} [cm^{-1}]
terrace	fcc	-2.18	1511	1490
step	bridge	-2.27	1630	1610
	lower fcc	-1.59	1480	1385
kink	bridge	-2.50	1620	
	lower fcc	-1.49	1460	

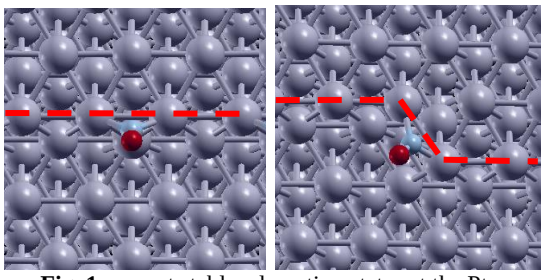

Fig. 1. most stable adsorption states at the Pt (a) step and (b) kink sites.

[1] N. Tsukahara et al., Surf. Sci. 600 (2006) 3560-3563. [2] N, Tsukahara et al., Surf. Sci. 600 (2006) 3477-3481.

PIIb-04

Computational Mutation Analysis of Diol Dehydratase in Glycerol Dehydration

Kazuki Doitomi[1], Takashi Kamachi[1], Tetsuo, Toraya[2] and Kazunari Yoshizawa[1]
[1]*Institute for Materials Chemistry and Engneering, Kyushu University*
Motooka, Nishi-ku, Fukuoka 819-0395, Japan
[2]*Graduate School of Natural and Technology, Okayama University*
Tsushima-naka, Kita-ku, Okayama 700-8530, Japan
e-mail address: dtomi@ms.ifoc.kyushu-u.ac.jp

I. Introduction

Diol dehydratase catalyzes the conversion of 1,2-diols into corresponding aldehydes. During the glycerol dehydration, the enzyme is subject to 'suicide inactivation'. Recently, Toraya and co-workers prepared the mutant enzymes of the Gln336Ala and Ser301Ala mutants, which are more resistant to the inactivation [1]. In this study, we investigated from QM/MM computations the inactivation mechanism of the wild-type enzyme and discuss why the inactivation is suppressed in the Gln336Ala and Ser301Ala mutants.

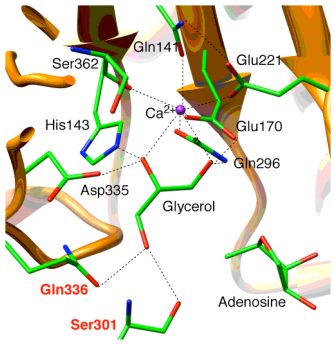

Fig. 1. Crystal structure of the active site.

II. Calculation methods

We build an entire model based on the crystal structure. The Gln336 and Ser301 residues were replaced by alanine in the mutants (Fig. 1). The ChemShell software was used to perform QM/MM calculations by integrating the TURBOMOLE package for QM (B3LYP/TZVP// B3LYP/SV(P)) and the DL-POLY program for MM with CHARMm force field.

III. Results

Fig. 2 shows the reaction mechanisms of the dehydration reaction and inactivation. Once glycerol is bound to the active site, the enzyme distinguishes two binding conformations (GS and GR). The OH group migration and hydrogen transfer take place competitively. The energy difference between the OH group migration and hydrogen transfer is 11.2 and 15.6 kcal/mol in the GS and GR conformation, respectively. Because of the smaller energy difference, the inactivation mainly proceeds in the GS conformation [2].

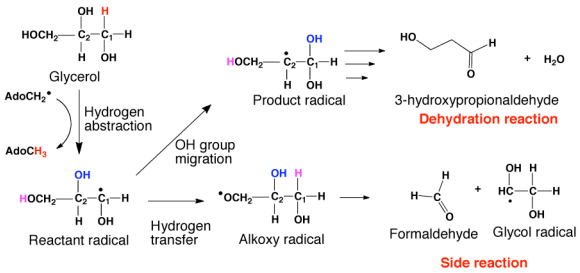

Fig. 2. A mechanism for dehydration reaction and inactivation

Key hydrogen-bonding interactions in the active site are found to be perturbed by the mutations [3]. The mutational analysis well explains the resistance to the inactivation in the mutants. The computational mutation approach would have a potential to assist the rational design of enzymes with new catalytic functions.

[1] Yamanishi, *et al. FEBS J.* **2012**, *279*, 793. [2] Doitomi, K.; Kamachi, T.; Toraya, T.; Yoshizawa, K. *Biochemistry* **2012**, *52*, 9202. [3] Doitomi, K.; Kamachi, T.; Toraya, T.; Yoshizawa, K *Chem. –Asian J. submitted*

PIIb-05

Double-QM/MM Method for Donor-Acceptor Electron Transfer Studies with Solvent Reorganization

Zdeněk Futera[1,2], Keitaro Sodeyama[2,3], Jaroslav V. Burda[4], Yoshitaka Tateyama[2,3,5]

[1]*Keio University, 3-14-1 Hiyoshi, Kohoku-ku, Yokohama 223-8522, Japan*

[2]*International Center for Materials Nanoarchitectonics (WPI-MANA), National Institute for Materials Science (NIMS), 1-1 Namiki, Tsukuba, Ibaraki 305-0044, Japan*

[3]*ESICB, Kyoto University,Goryo-Ohara, Kyoto 615-8245, Japan*

[4]*Charles University in Prague, Ke Karlovu 3, 121 16 Prague 2, Czech Republic*

[5]*PRESTO and CREST, Japan Science and Technology Agency (JST), 4-1-8 Honcho, Kawaguchi, Saitama 333-0012, Japan*

E-mail address: FUTERA.Zdenek@nims.go.jp

Electron transfer (ET) processes play important role in many physical and chemical phenomena such as catalysis, corrosion or photosynthesis and their detailed knowledge is desirable for construction of full cells or solar cells. We developed a double-QM/MM (d-QM/MM) computational method with a novel concept of multiple QM regions designed for investigation of donor-acceptor ET in condensed matter. The full reaction computational scheme of ET reaction is accessible with d-QM/MM that allows exploring D-A distance dependency of the ET process while the spin-charge state and appropriate exchange-correlation treatment of DA sites can be easily controlled. This is especially important for metallic DA centers that are most common.

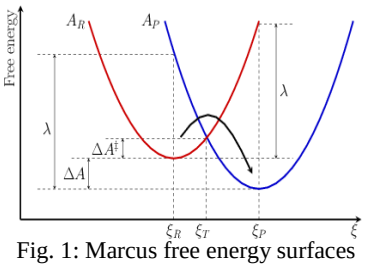

Fig. 1: Marcus free energy surfaces

$$\lambda(R_{DA}) = \left(\frac{1}{\varepsilon_0} - \frac{1}{\varepsilon_s}\right)\left(\frac{1}{2r_D} + \frac{1}{2r_A} - \frac{1}{R_{DA}}\right)(\Delta q)^2 \quad (1) \qquad k(T) = \frac{2\pi}{\hbar}\frac{|V_{DA}|^2}{\sqrt{4\pi\lambda k_B T}}\exp\left[-\frac{(\lambda+\Delta A)^2}{4\lambda k_B T}\right] \quad (2)$$

We demonstrate accuracy and performance of d-QM/MM method on model self-exchange ET reaction between $Fe^{2/3+}$ cations in water as well as on heterogeneous ET in Fe^{2+} + Ru^{3+} pair in the same medium. We employ Marcus theory in linear response approximation together with MD sampling techniques to calculate distance dependent redox free energy ΔA, and reorganization free energy λ of the reaction using DFT with hybrid B3LYP and high spin state description of iron centers. While ΔA, as a property of DA electronic states, is constant above touching sphere limit, λ is increasing to its dilute limit value according to Marcus formula (Eq. 1). Finally, to estimate rate constant of the ET process (Eq. 2), we calculated electronic coupling in two-state approximation between HOMO of donor and LUMO and acceptor. The coupling is linearly dependent on MO overlap integral and it decays exponentially to zero beyond the touching sphere limit. Based on these results, we can conclude that d-QM/MM method has a potential to be a powerful tool for investigation of large variety of ET processes, especially reactions on solid/liquid interfaces

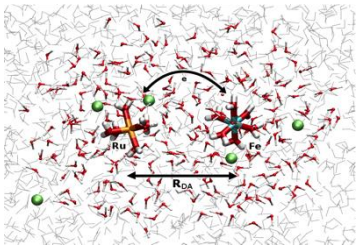

Fig 2: Fe^{2+}-Ru^{3+} ET reaction model

PIIb-06

Application of Ewald Sum for ONIOM method

Osamu Kobayashi and Nanbu Shinkoh
Department of Materials and Life Sciences, Faculty for Science and Engineering, Sophia University, Kioicho,Chiyoda-ku, Tokyo,102-8554, Japan

I. Abstract

Morokuma et al. have proposed one of sophisticated approaches in combined quantum mechanical and molecular mechanical (QM/MM) method for treating the large chemical system; that is ONIOM (our Own N-layer integrated molecular Orbitals and molecular Mechanics) theory[1]. The ONIOM energy expression is written as an extrapolation.

$$E_{\mathrm{ONIOM}} = E^{\mathrm{MM}}_{\mathrm{real}} + E^{\mathrm{QM}}_{\mathrm{model}} - E^{\mathrm{MM}}_{\mathrm{model}}$$

In this paper we present the method to combine ONIOM method and particle mesh Ewald summation (ONIOM-PME) method. We applied this method to simulate the non-adiabatic transition of protonated Schiff base (PSB). Here, PSB3 is known as model molecule of retinal, which changes its conformation via non-adiabatic process (Fig. 1). In our simulation, non-adiabatic transition is taken account with molecular dynamics (MD) simulation with trajectory surface hopping (TSH) method.

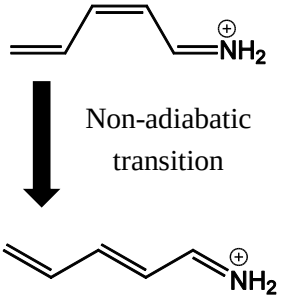

Fig 1. Non-adiabatic conformational change in PSB3

II. Computational Details

The model and real layers define the unit cell and PSB3 cation. Image layer defines the periodic replica of the real layer. For QM calculation, complete active space (6e, 6o) self-consistent field (CASSCF) method with MIDI4* (split valence-type) basis set was employed. The charge of unit cell was taken account of QM calculation with electronic embedding scheme. All QM calculation was performed with Molpro 2012. For MM calculation, general AMBER force field (GAFF) and restricted electrostatic potential (RESP) charge was employed. The force field was generated with Leap and ANTECHAMBER, which are available in AMBER 9 program package. The energy and force was calculated with our original program.

III. Results

In the MD simulation with ONIOM-PME method, it takes longer time to transit to S_0 via non-adiabatic transition than traditional ONIOM approach. We consider this effect derives from solvent effect. The preceding experiment by El-Sayed et. al.[2] shows non-adiabatic transition in solvent becomes slower than in gas phase and in protein, and indicates non-adiabatic transition is affected by solvent motion. Our calculation is consistent to their result.

[1] K. Morokuma et. al., *WIREs Comput Mol Sci*, **2011,** 1-24
[2] El Sayed et. al., *J. Phys. Chem.* **1996,** 100-18586-18591

PIIb-07

3D-RISM-SCF Analysis of the Solvent Effect on the Electronic Structures of Merocyanines

Yuichi Tanaka, Norio Yoshida, and Haruyuki Nakano
Department of Chemistry, Graduate School of Sciences, Kyushu University,
Hakozaki, Higashi-ku, Fukuoka 812-8581, Japan
e-mail address: ta-chan@ccl.scc.kyushu-u.ac.jp

Merocyanines exhibit solvatochromism, the color change of the solution depending on the solvent. The magnitude of solvatochromic shift can be qualitatively explained from the macroscopic physical quantity such as dielectric constant of the solvent. However, to understand and control the chromism from a microscopic viewpoint, studies on the solvent effect based on molecular theory are crucial. In the present study, we investigate the excitation energies of streptopolymethinemerocyanine (SPMC; $H_2N(C_2H_2)_nCHO$ (n = 1-8); Figure 1) and solvent effect on them using the three-dimensional reference interaction site model self-consistent field (3D-RISM-SCF) method. Since the electronic structures of the solute molecule depend on the environment and the conjugated chain length, we focus on the solvent and chain length dependencies of the excitation energies.

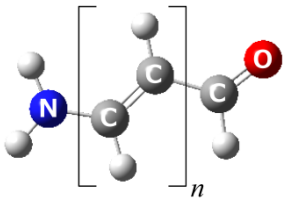

Fig. 1 SPMC

Figure 2 shows the π-π* and n-π* excitation energies against the chain length n. The method of the calculations was LC-TD-BOP/aug-cc-pVDZ and the solvents examined were water, methanol, and acetonitrile. Noteworthy are following three points. First, at small n chain length, the π-π* excitation energies exhibit red shifts by solvation regardless of the solvent, while the n-π* excitation energies exhibit blue shifts. Second, the order of the magnitudes of the shifts in both the π-π* and n-π* excitation energies are water > methanol > acetonitrile at small n chain length. Third, the shift direction in the π-π* excitation energy in acetonitrile changes with the extension of the chain length. To understand these points, we computed the electrostatic potential (ESP) due to the solvent along the solute molecule (more specifically, ESP at the N, C, and O atoms). The results showed clear difference between the protic (water and methanol) and aprotic (acetonitrile) solvents. In particular, the difference in the chain-length dependency is noticeable. The points above can be understood using the ESPs. For example, the first point is explained from the interaction between the SPMC dipole moments in the ground and excited states and the ESP made by the solvent molecules. These results indicate that the microscopic knowledge of the solvent distribution is essential for the understanding of the solvatochromic shifts of SPMC, as well as the macroscopic knowledge such as dielectric constants.

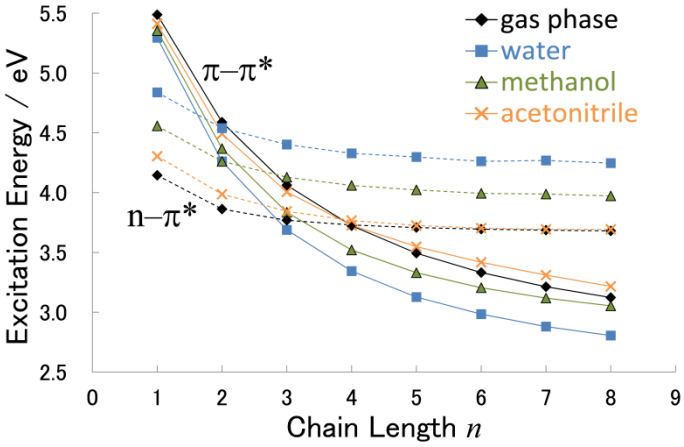

Fig. 2 π-π* and n-π* excitation energies of SPMC

PIIb-08

Electrolyte-Dependent Characteristics of the Solid Electrolyte Interphase Film Formation in the Lithium-Ion Batteries

Norio Takenaka[1,2], Yuichi Suzuki[1], Hirofumi Sakai[1] and Masataka Nagaoka[1,2]
[1]*Graduate School of Information Science, Nagoya University, Furo-cho, Chikusa-ku, Nagoya 464-8601, Japan*
[2]*ESICB, Kyoto University, Katsura, Nishikyou-ku, Kyoto 615-8520, Japan*
e-mail address: takenaka@ncube.human.nagoya-u.ac.jp

I. Introduction

The performance of current lithium-ion battery (LIB) with liquid electrolytes, e.g., ethylene carbonate (EC) and propylene carbonate (PC), strongly depends on the formation of stable solid electrolyte interphase (SEI) film on the anode surface, which is formed as a result of reduction of the electrolyte. Despite the close structural similarity between EC and PC, it is not clear why the SEI film becomes unfavorable only in the PC-based electrolyte.

II. Method

To investigate such electrolyte dependent characteristics of the SEI film formation, we have performed the atomistic reaction simulations with the recently developed hybrid Monte Carlo (MC)/molecular dynamics (MD) reaction method [1]. The present atomistic reaction simulations were executed in 1.1 mol/L $LiPF_6$ EC- and PC-based electrolytes with the graphite anode, where the computational model and the reaction scheme consisting of list of elementary reaction processes are shown in Figure 1.

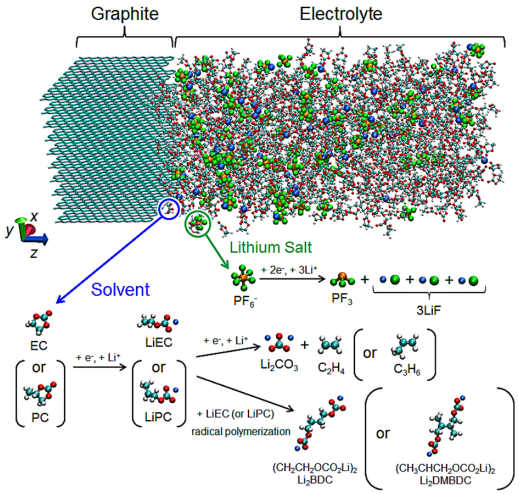

Fig.1 Simulation model and elementary reaction processes

III. Results and Discussion

In the resulting SEI films, it was found that the inorganic salts (e.g. Li_2CO_3) tend to deposit closer to the graphite anode, while the organic ones (e.g. Li_2BDC, Li_2DMBDC) mainly do in the outer layer as is the same in the experimental observations (see Figure 2). We also found that the dense EC-based SEI film can protect the electrolyte from the reduction. In contrast, the PC-based one became sparse and could not protect the electrolyte. This is considered because that the methyl groups in the solvent PC molecules and their reaction products prevent the organic salts from aggregating during the SEI film formation processes [2].

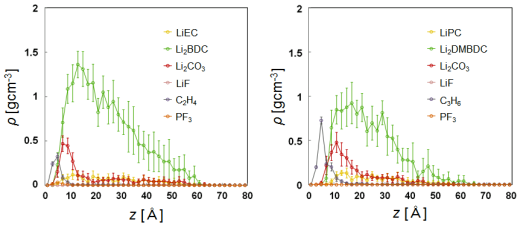

(a) EC-based electrolyte (b) PC-based electrolyte

Fig.2 Mass density distributions of SEI films

[1] M. Nagaoka, Y. Suzuki, T. Okamoto, N. Takenaka, *Chem. Phys. Lett.*, **583**, 80 (2013).
[2] N. Takenaka, Y. Suzuki, H. Sakai, M. Nagaoka, to be submitted.

PIIb-09

Intramolecular Electron Transfer in Polar Solvents Calculated by Constrained Density Functional Theory

Satoshi Muraoka and Kenji Morihashi
University of Tsukuba
Tennoudai, Tsukuba-shi, Ibaraki, 305-8571, Japan
e-mail address: muraoka@dmb.chem.tsukuba.ac.jp

Ⅰ. Introduction

Dinitroaromatic radical anions were the first symmetrical organic mixed valence (MV) compounds for which intramolecular electron transfer (IET) reactions were studied by electron spin resonance (ESR) spectroscopy. Values of IET rate constant (k_{ET}) are varied by the various polar solvents. In this study, we estimated the reorganization energy and the electronic coupling matrix element incorporating a direct interaction between solute and solvent molecules. These parameters were calculated by constrained density functional theory (CDFT)[1]. The values of k_{ET} were determined on the basis of Marcus theory.

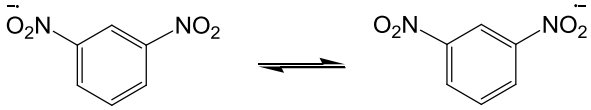

Fig.1 IET reaction on *m*-dinitrobenzene (*m*-DNB)

Ⅱ. Computational detail

m-dinitrobenzene (*m*-DNB) is one of the organic MV compounds which cause IET reaction. We made 14 models; one solvent acetonitrile (MeCN) around one solute *m*-DNB (Fig.1). The methyl group of MeCN is present on the side of *m*-DNB in ①~⑦, and the cyano group is present on the side of that in ⑧~⑭. The distance between the solute- and solvent-molecules varies from 3.0 to 6.0 Å by 0.5 Å in each configuration. The CDFT calculation was carried out for each configuration using B3LYP/6-31G(d).

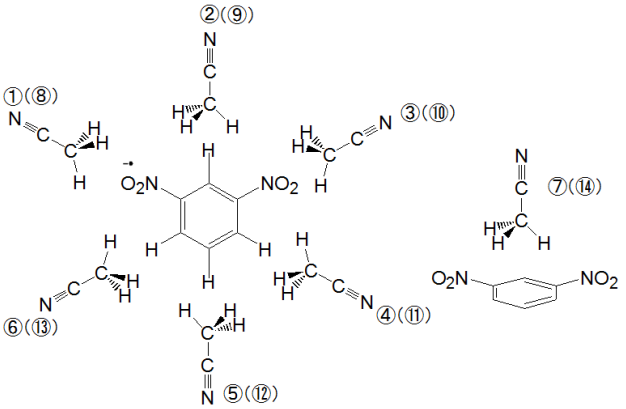

Fig. 2 14 models

Ⅲ. Result

The configuration of ① ~ ⑦ is relatively stable. On the other hand, that of ⑧~⑭ is very unstable. The most stable configuration is ① (R = 4.0 Å). The value of k_{ET} is the smallest in ① and is the largest in ③.

Table 1 k_{ET} of ① and ③

		①(R = 4.0 Å)	③(R = 4.0 Å)	vac	explt[2]
k_{ET}	[s^{-1}]	7.87×10^{8}	2.30×10^{13}	2.09×10^{11}	4.63×10^{10}
log k_{ET}		8.90	13.36	11.32	10.67

[1] Q. Wu, T. Van Voorhis, *J. Chem. Theo. Comput.,* **2006**, 2, 765.

[2] H. Hosoi, Y. Masuda, *J. Mol. Liq.* **2001,** 90, 279.

PIIb-10

Synthesis of Antimalarial of 1,10-Phenanthrolinium Bromide Derivatives from Clove and Wintergreen Oils

Dhina Fitriastuti, Muhammad Idham Darussalam Mardjan, Jumina and Mustofa
Department of Chemistry, Universitas Gadjah Mada, Yogyakarta, 55281, Indonesia
e-mail address: dhinafitriastuti@yahoo.co.id

Abstract

The synthesis of antimalarial compound of 1,10-phenanthrolinium bromide derivatives had been conducted from clove and wintergreen oils. The 1,10-phenanthroline derivatives were designed and synthesized from vanillin (which could be derived from clove oil) and methyl salicylate (which could be derived from wintergreen oil) as the main raw material. In addition, development of the synthesis method by using *green* method were evaluated also.

The first step of reaction was made various of benzaldehydes from clove and wintergreen oils as starting material. The various of benzaldehydes were reduced using sodium borohydride ($NaBH_4$) with grinding method and yielded benzyl alcohols. Benzyl alcohols were brominated using PBr_3 to yield benzyl bromides. The final step was benzylation of 1,10-phenanthroline monohydrate with benzyl bromides under reflux condition in acetone for 14 h to afford various of 1,10-phenanthrolinium bromide derivative. The structures of products were characterized by IR, GC-MS and ^{1}H-NMR spectrometers.

The products of synthesis were (1)-N-(3,4-dimethoxybenzyl)-1,10-phenanthrolinium bromide and (1)-N-(4-ethoxy-3-methoxybenzyl)-1,10-phenanthrolinium bromide from clove oil and (1)-N-(2-methoxybenzyl)-1,10-phenanthrolinium bromide from wintergreen oil.

Keywords: Clove oil, wintergreen oil, derivatives of 1,10-phenanthrolinium bromide, antimalarial

PIIb-11

The oxidative addition of chlorobenzene on bimetallic Au/Pd catalysts: An DFT study

Bundet Boekfa [1,2], Masahiro Ehara [1], Jumras Limtrakul [2], Raghu Nath Dhital [1] and Hidehiro Sakurai [1]

[1]*Research Center for Computational Science, Institute for Molecular Science, Myodaiji, Okazaki 444-8585, Japan*

[2]*Department of Chemistry, and NANOTEC Center for Nanoscale Materials Design for Green Nanotechnology, Kasetsart University, Bangkok 10900, Thailand.*

e-mail address: ehara@ims.ac.jp

I. Introduction

Heterogeneous coupling reaction is an important strategy for the organic synthesis. Recently, various type of catalytic reactions have been achieved with gold nanoparticles or gold/palladium alloy nanoparticles supported by metal oxides or polymers [1]. In these reactions, the oxidative addition is an key step because the reaction starts from this process [2]. In this work, the oxidative addition of chlorobenzene over $Au_{10}Pd_{10}^-$ clusters has been theoretically investigated with density functional theory (DFT). We have examined the various models for $Au_{10}Pd_{10}^-$ clusters and calculated the oxidative addition process at various adsorption sites.

II. Methodology

The oxidative addition of chlorobenzene over Au/Pd Catalysts was calculated by the DFT calculations with M06 functional. All structures were fully relaxed in the geometry optimization without any constraint. The Au and Pd atoms were treated by relativistic ECP with double-ζ basis set [3s3p3d] (LANL2DZ), while the 6-31G(d,p) basis set was adopted for H, C and Cl atoms. All calculations were calculated using the Gaussian 09 program.

III. Results

First, we optimized various structural isomers for $Au_{10}Pd_{10}^-$ clusters. The most stable structure is similar to that obtained with Gupta potential calculation [3]. The spin density isosurface has been shown in Fig 1. The various positions were examined for the oxidative addition of chlorobenzene. We found that the reaction on $Au_{10}Pd_{10}^-$ cluster should occur at Pd site (ΔE=-31.2 kcal/mol, E_a=21.0 kcal/mol) rather than Au site (ΔE= -26.3 kcal/mol, E_a=26.4 kcal/mol). For the neutral cluster, $Au_{10}Pd_{10}^0$, the adsorption and activation energies are similar to anion cluster. (ΔE=-35.9 kcal/mol, E_a=22.4 kcal/mol).

The stability, adsorption energy, and activation energy barrier at various sites of some isomers will be discussed in the presentation.

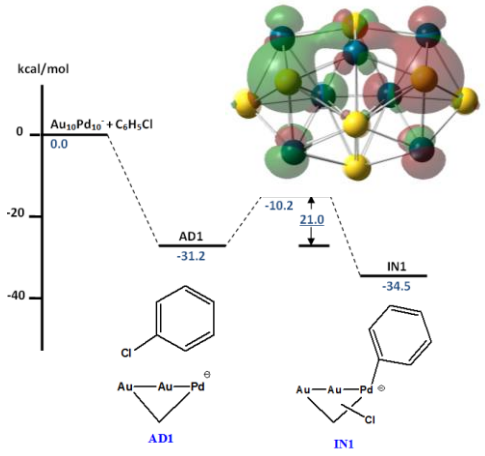

Fig. 1. Energy diagram of the oxidative addition of chlorobenzene on $Au_{10}Pd_{10}^-$ cluster with spin density of the cluster.

[1] T. Tsukuda, H. Tsunoyama, H. Sakurai, *Chem. Asian J*, **2011**, 6, 736-748. [2] R.N. Dhital, C. Kamonsatikul, E. Somsook, K. Bobuatong, M. Ehara, S. Karanjit and H. Sakurai, *J. Am. Chem. Soc.* **2012**, 134, 20250-20253. [3] F. Pittaway, L.O. Pza-Borbon, R.J. Johnston, H. Arsland, R. Ferrando, C. Mottet, G. Barcaro and A. Fortunelli, *J. Phys Chem C.* **2009**, 113, 9141-9152.

PIIb-12

Theoretical investigation on poly-*para*phenylenevinylene (PPV) charge transfer process

AIKAWA Koharu, and MORIHASHI Kenji
Graduate School of Pure and Applied Sciences, University of Tsukuba,
Tenodai 1-1-1, Tsukuba, Ibaraki 305-8571, Japan
e-mail address: aikaw@dmb.chem.tsukuba.ac.jp

I. Introduction

PPV, one of OLED materials, has an interesting electron-transfer (ET) process between the electron-donor (D) and acceptor (A), which induces an electro-luminescence phenomenon. We studied the ET process (Figure 1) theoretically, and investigated how the ET rate constant varies with the inter-rotational angle of the donor (or acceptor) site in the D-A complex.

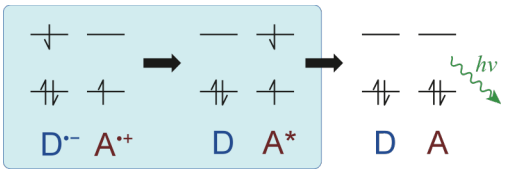

Figure 1. Electron transfer process in the electroluminescence.

II. Computational detail

PPV is a polymer system, and we used 3 units oligo-PV (OPV3) for the model system. OPV3 was optimized at the B3LYP/6-31G(d) level. First, the two OPV3 sites were put so as to be cofacial orientation, where the site-site distance is at 2.9 Å. And then, either the donor or acceptor site was rotated around its principal axis of inertia. Secondly, we changed the site-site distance, while the inter-rotational angle was fixed at 45°. To calculate the ET rate constants, we used the 4-point method on the basis of Marcus theory. We have calculated the OPV3 dimer system with constrained DFT (CDFT) method [1,2] at the B3LYP/6-31G(d) level. The constrained value of initial electron state $\{D^{\bullet-}\ldots A^{\bullet+}\}$ is 2.0 for the charge density, and of final state $\{{}^1D\ldots{}^3A^*\}$ is 2.0 for the spin density.

III. Result

The ET rate constant of OPV3 is completely different between the acceptor- and donor-rotated configurations. The acceptor-rotated configurations have higher in ET rate constant than the donor-rotated ones (Figure 2). Similarly, at the acceptor-rotational angle of 45°, the rate constant varies higher as the site-site distance decreases. By contrast, at the donor rotational angle of 45°, the rate constant is lower with the shorter site-site distance.

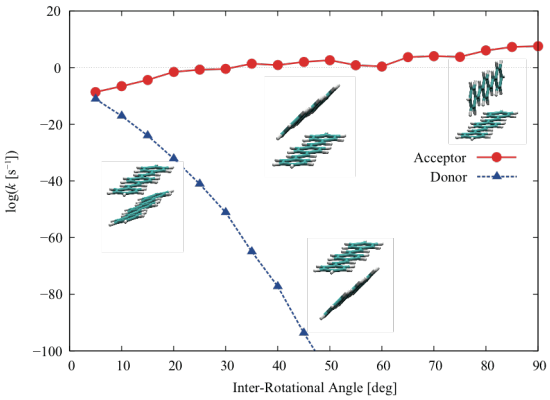

Figure 2. Electron-transfer rate constant versus inter-rotational angle. Red filled circles are acceptor rotation, and blue filled triangles are donor rotation.

[1] Q. Wu and T. Van Voorhis, J. Chem. Theory Comput. **2**, 765 (2006).
[2] B. Kaduk, T. Kowalczyk, and T. Van Voorhis, Chem. Rev. **112**, 321 (2012).

PIIb-13

First-principles Calculation of Suzuki-Miyaura Cross Coupling Reaction by Palladium Catalyst

Daisuke Mimura[1], Atuya Takeda[1], Susumu Yanagisawa[2], Kouji Inagaki[1], Yoshitada Morikawa[1] and Takashi Ikeda[3]

[1] *Department of Precision Science and Technology, Graduate School of Engineering, Osaka University, Suita, Osaka 565-0871, Japan*

[2] *Department of Physics and Earth Sciences, Faculty of Science, University of the Ryukyus, Okinawa 903-0129, Japan*

[3] *Japan Atomic Energy Agency, Sayougun, Hyougo 679-5148, Japan*

e-mail address: mimura@cp.prec.eng.osaka-u.ac.jp

I. Introduction

Suzuki-Miyaura reaction is one of the most important reactions in modern organic synthesis. Suzuki-Miyaura reaction uses Pd catalyst, so many kind of Pd catalysts have been reported. One of the most promising catalysts is "intelligent catalyst[1]" that exhibits highly active performance in Suzuki-Miyaura reaction[2]. But the reason why this catalyst has highly active performance has not been clarified. In this research, we try to clarify the mechanism of catalytic reactions by comparing the free energy barriers for oxidative addition of the intelligent catalyst with that of conventional catalyst by using first-principles molecular dynamics simulations.

II. Results and Discussion

As a model of conventional catalyst, we employed $PdPPh_3$ since the reaction occurs after PPh_3 dissociation from $Pd(PPh_3)_2$ and as a model of the intelligent catalyst, we employed Pd atom coordinated by two H_2O molecules since Pd atoms are dissolved into solution from the intelligent catalyst. We carried out Blue Moon Ensemble simulation using these catalysts for a process in which Pd is inserted in between Br and C of bromobenzen, i.e. the oxidative addition. The figure shows the structures of transition states of the two cases ((a) $PdPPh_3$, (b) Pd with water). We found the free energy barriers are about 0.11eV for $PdPPh_3$ and 0.08eV for Pd in water. The free energy difference between two catalysts is small. Usually, conventional Pd catalyst has two ligands like $Pd(PPh_3)_2$. When $Pd(PPh_3)_2$ is inserted in between C and Br there is large steric effect because of bulky ligands and it is necessary to dissociate one ligand. On the other hand, two H_2O coordinate to a Pd atom as ligands in water and there is small steric effect because H_2O is less bulky than PPh_3. This difference leads to the difference in the catalyitic reactivity.

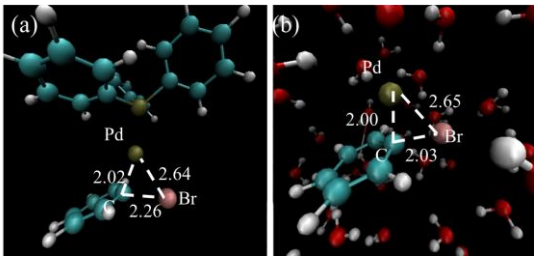

[1]Y. Nishihata, et al, Nature. 418, 164-167(2002)
[2]S. P. Andrews, et al, Adv. Synth. Catal. 347, 647-654 (2005)

PIIb-14

First-principle simulations for matrix-isolation vibrational spectra of noble gas compounds: applications to HXeCl and XeBeO

Keisuke Niimi, Akira Nakayama, Yuriko Ono, Tetsuya Taketsugu
Graduate School of Chemical Sciences and Engineering, Hokkaido University,
Kita 13, Nishi 8, Kita-ku, Sapporo, Hokkaido 060-8628, JAPAN
e-mail address: niimi@mail.sci.hokudai.ac.jp

I. Introduction

We investigate the vibrational shift of beryllium oxide (BeO) in Xe matrix as well as in Ar matrix environments by mixed quantum-classical simulation and examine the origin of spectral shift in details. BeO is known to form strong chemical complex with single rare gas atom [1], and it is predicted from the gas phase calculations that vibrational frequencies are blue-shifted by 78 cm^{-1} and 80 cm^{-1} upon formation of XeBeO and ArBeO, respectively. However, this shift in XeBeO (ArBeO) complex is larger than that observed in the Xe (Ar) matrix experiments, which was about 34 (62) cm^{-1} [2], and it is anticipated that the effect of surrounding media may not be negligible. In this study, we examine the origin of spectral shift in details from the viewpoints of complex-formation and perturbations from surrounding atoms. Furthermore, we also investigarte the vibrational shift of HXeCl in Xe, Ar and Ne matrices, where H-Xe stretching vibrational frequency is experimentally reported[3-4].

II. Computational method

We use the hybrid quantum-classical Hamiltonian that is assumed to have the following pairwise-additive form:

$$H = \sum_{i=1}^{N_q} \frac{1}{2}\hat{p}_i^2 + \sum_{i=1}^{N} \frac{1}{2}\mathbf{P}^{(i)} + V_{\mathrm{qm}}(\hat{\mathbf{q}}) + \sum_{i=1}^{N} V_{\mathrm{qm\text{-}Rg}}(\hat{\mathbf{q}}, \mathbf{R}^{(i)}) + \sum_{i<j}^{N} V_{\mathrm{Rg\text{-}Rg}}(|\mathbf{R}^{(i)} - \mathbf{R}^{(j)}|) \qquad (1)$$

where **q** and **p** represent the normal coordinates and their conjugate momenta of RgBeO (Rg = Xe or Ar), and **R** and **P** are the coordinates and momenta of rare gas atoms respectively. In this work, all interaction potentials are evaluated by *ab initio* calculations at the level of CCSD(T). The vibrational energy levels of RgBeO in the presence of surrounding Rg atoms are obtained by the PO-DVR method. The Monte Carlo simulations are performed to sample the configurations of rare gas atoms around RgBeO.

III. Results

When the effects of other surrounding rare gas atoms are included by Monte Carlo simulations, it is found that the vibrational frequencies are red-shifted by 21 cm^{-1} and 8 cm^{-1} from the isolated XeBeO and ArBeO complexes, respectively(see Fig.1). The calculated vibrational frequency shifts from the isolated BeO molecule are in reasonable agreement with experimental values[5].

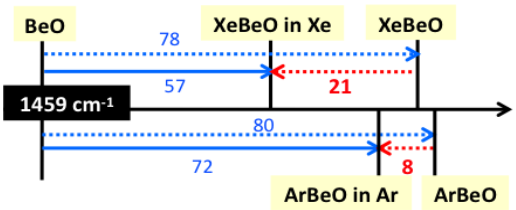

Fig.1: The vibrational shift of XeBeO and ArBeO in Xe and Ar matrices, respectively [cm^{-1}]

References

[1] A. Veldkamp and G. Frenking, Chem. Phys. Lett. **226**, 11 (1994).
[2] C. A. Thompson and L. Andrews, J. Am. Chem. Soc. **116**, 423 (1994); J. Chem. Phys. **100**, 8689 (1994).
[3] M. Pettersson, J. Lundell, and M. Räsänen, J. Chem. Phys. **102**, 6423 (1995).
[4] M. Lorenz, M. Räsänen, and V. E. Bondybey, J. Phys. Chem. A **104**, 3770 (2000).
[5] A. Nakayama, K. Niimi, Y. Ono, and T. Taketsugu, J. Chem. Phys. **136**, 054506 (2012).

PIIb-15

Low-temperature Excess Heat Capacity of Potassium Germanate Glasses

Seiichi Mamiya
Graduate School of Pure and Applied Sciences, University of Tsukuba,
Tennodai, Tsukuba, Ibaraki, 305-8573, Japan
e-mail address: mamiya@ims.tsukuba.ac.jp

I. Purpose

The purpose is to measure the low-temperature heat capacity of potassium germanate glass, propose a model to explain an excess heat capacity and clarify its origin [1].

II. Experimental

Five samples of potassium germanate glasses (xK$_2$O·(100-x)GeO$_2$: x indicates K$_2$O content mol%) x=0, 10.1, 19.0, 28.2, 39.0 were prepared by the solution method. The capacities of samples were measured in the temperature range from 2 to 50 K.

III. Results and Discussion

Fig. 1 shows the reduced excess heat capacity (C_pT^{-3}) with the temperature (T) of each sample. A curve of the GeO$_2$ glass crosses those of the other three glasses. This is a queer phenomenon in regular capacity change. This may be an interaction between isolated structural units and a main network structure, because the other factor of heat capacity is the interaction. In addition, a minimum value among maximum C_pT^{-3}s of all samples occurs at x=15 (Fig. 2). At the same K$_2$O content the elastic modulus shows a maximum value. The relationship between the C_pT^{-3} and the elastic modulus is clarified by theories of liquid and the results of Raman scattering experiment.

IV. Conclusion

The theories of liquids explain the excess heat capacity of glass is caused by the interaction between the isolated structural units and the main network structure more understandably.

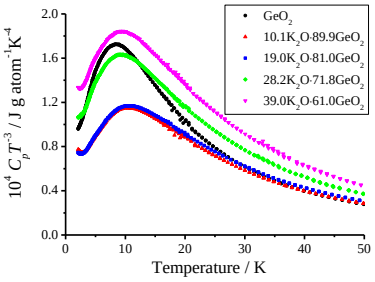

Fig.1. The temperature dependence of C_pT^{-3} of potassium germanate glasses.

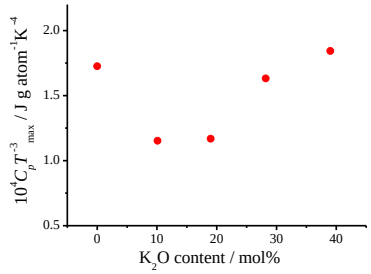

Fig. 2. The content dependence of maximum reduced excess heat capacity $C_pT^{-3}_{max}$ of potassium germanate glasses.

[1] S. Mamiya, *Modern Applied Science*, **7**(5) (2013) 22 doi:10.5539/mas.v7n5p22.

PIIb-16

Effect of the donor-π-donor type charge distribution on the second hyperpolarizabilities of open-shell singlet systems – *para*-quinodimethane with point charge model

Kotaro Fukuda and Masayoshi Nakano
Graduate School of Engineering Science, Osaka University,
1, Machikaneyama-cho Toyonaka, Osaka 560-8531, Japan
e-mail address: k-fukuda@cheng.es.osaka-u.ac.jp

I. Introduction

Molecular design for the nonlinear optical (NLO) material has been extensively investigated because of their potential applications in future photonics and optoelectronics. Recently, we have found that the second hyperpolarizabilities γ, which is an origin of the third order NLO phenomena, has a strong dependence on the diradical character *y*, which is an index of the open-shell nature taking a value between 0 (closed-shell) to 1 (pure open-shell), and takes a maximum around the intermediate *y* value, i.e. *y*–γ correlation [1]. According to this new guideline, we have designed several NLO molecules. On the other hand, several investigations on the closed-shell systems have revealed that the emergence of the quadrupole type charge distribution like donor–π–donor (D–π–D) nature enhances the NLO properties [2], while this effect on the systems with several open-shell singlet natures are still within the veil.

In this study, we consider the *para*-quinodimethane with point charge model (PQM-pc) (Figure 1), in which we place the point charges at 2.0 Å away from the exocyclic carbon atom on both sides of the PQM model [1] in order to investigate the D–π–D type charge distribution effect on the NLO properties of the open-shell singlet systems with different diradical characters.

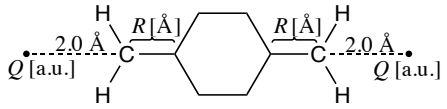

Figure 1. Structure of the PQM with point charge model (Q = 0, -1, -2, -3, R = 1.35 – 2.20)

II. Results and discussion

Figure 2 shows the sum of the natural charges of the central benzene ring q_c according to the absolute value of each point charge, which is regarded as an index of the D–π–D nature. It is found that q_c is, at first, quite small when no point charge is placed, and the presence of the external point charge increases the q_c value, which shows an almost linear dependence on the absolute value of the point charge Q. These observations indicate that the present model mimics the D–π–D systems, where the degree of the D–π–D nature increases with the absolute value of the external point charge. In the poster session, details of the relationship between the D–π–D nature, the diradical character and the second hyperpolarizabilities will be presented.

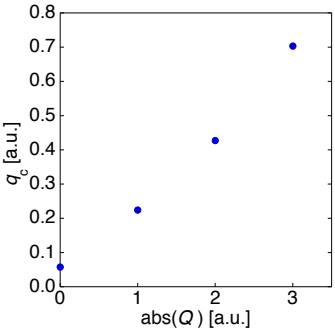

Figure 2. Natural charge of the central benzene ring q_c [a.u.] for each absolute value of point charge Q [a.u.].

[1] M. Nakano et al., *J. Phys. Chem. A* **109**, 885 (2005); *Phys. Rev. Lett.* **99**, 033001 (2007); *J. Chem. Phys.* **133**, 154302 (2010); *J. Chem. Phys.* **138**, 244306 (2013).
[2] M. Albota et al., *Science* **281**, 1653 (1998).

PIIb-17

Computational Molecular Spectroscopy of ZnOH: Comparison with FeOH and CsOH

Umpei Nagashima[1], Tsuneo Hirano[1,2]

[1] *Nanosystem Research Institute (NRI), National Institute of Advanced Industrial Science and Technology (AIST), 1-1-1 Umezono, Tsukuba, Ibaraki 305-8568, Japan.*

[2] *Ochanomizu University, 2-1-1 Otsuka, Bunkyo-ku, Tokyo 112-8610, Japan.*

e-mail address: u.nagashima@aist.go.jp

Table 1. Molecular constants of ZnOH

	Calc.	Exp. Zack (2012)	error
A_0 /MHz	763289	745084(1800)	2.4%
B_0 /MHZ	11188.3	11163.4978(51)	0.2%
C_0 /MHz	10999.4	10971.5173(51)	0.3%
r_0(Zn-O) / Å	1.8078	1.8095(5)	0.09%
r_0(O-H) / Å	0.9778	0.964(7)	1.4%
$\angle_0$(Zn-O-H) / deg.	117	114.1(5)	
ω_1 (OH str.) /cm^{-1}	3855		
ω_2 (bend) /cm^{-1}	695		
ω_3 (Zn-O str.) /cm^{-1}	627		
ν_1 (OH str.)/ / cm^{-1}	3677		
ν_2 (bend) / cm^{-1}	665		
ν_3 (Zn-O str.) / cm^{-1}	616		

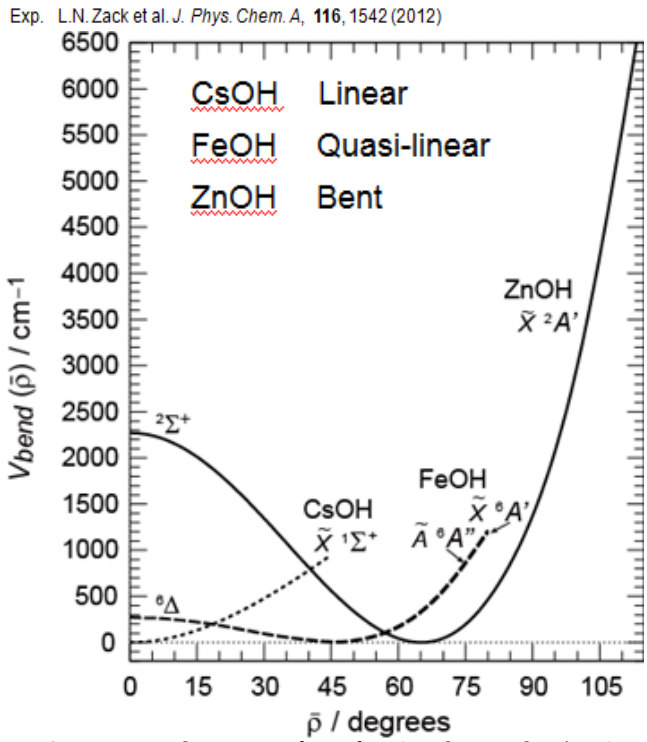

Fig. 1. Potential energy surface of ZnOH along with ∠ZnOH

Molecular geometry and molecular constants of ZnOH were very accurately computed with MRSDCI+Q /QZP ANO-RCC level of theory. Relativistic effect is also evaluated by DK3 level. Active space for MRSDCI is taken as valence: Zn 4s, 4p; O 2s, 2p; H 1s with Zn 3d dynamical electron correlations. Result is listed in Table 1.

Because Zn-O bond of ZnOH is almost ionic but has larger covalency than FeOH[1] and CsOH[2], molecular geometry of ZnOH is vent structure. Potential energy surface is depicted in Fig. 1 with those of FeOH (quasi -linear) and CsOH (linear).

Yamada-Winnewisser index[3] is useful to evaluate qualitatively geometry of tri-atomic molecule.

[1] T. Hirano, V. Derpmann, U. Nagashima, P. Jensen, J. Mol. Spectrosc., **263**, 150 (2010).

[2] T. Hirano, U. Nagashima, G. Winnewisser, P. Jensen, J. Chem. Phys., **132**, 094303 (2010).

[3] K. Yamada, M. Winnewisser, Z. Naturforsch., **31a**, 139 (1976).

PIIb-18

A SAC-CI study of the electronic excitation spectra of the radical anions and cations of azobenzene, stilbene, and benzalaniline

Yung-Ching Chou[1,2] and Hiroshi Nakatsuji[3]

[1.] *short-term research in Quantum Chemistry Research Institute,Japan*
[2.] *Department of Applied Physics and Chemistry,University of Taipei, No. 1, Ai-Guo West Road,Taipei 10048, Taiwan*
e-mail address: ycchou@utaipei.edu.tw
[3.] *Quantum Chemistry Research Institute, Kyodai Katsura Venture Plaza 106, Goryo Oohara 1-36,Nishikyo-ku, Kyoto 615-8245, Japan*

Abstract

The electronic excitation spectra of the radical anions and cations of azobenzene (trans and cis), stilbene (trans and cis) and benzalaniline (trans) were studied using SAC-CI theory. SAC-CI theory is a powerful tool to study the electronic excitation spectra of the radical anions and cations and is capable of describing the chemical properties of electronically excited states. The calculated transitions presented in this study agree with the experimental spectra.[1] The calculated transitions and the properties of the low-lying electronic excited states of the anions and cations of azobenzene, stilbene, and benzalaniline are discussed in this work.

[1] T. Shida, Electronic Absorption Spectra of Radical Ions, Physical Sciences Data Vol. 34 (Elsevier, Amsterdam, 1988) ISBN 0-444-43035-0.

PIIb-19

Theoretical study of the bimetal effect for CO adsorption at Ag islands on Ni(111)

Yuji Mahara, Junya Ohyama, Kyoichi Sawabe, Atsushi Satsuma
Graduate School of Engineering, Nagoya University
Furo-cho, Chikusa-ku, Nagoya-shi, Aichi-ken, 464-8603, Japan.
e-mail address: mahara.yuji@e.mbox.nagoya-u.ac.jp

I. Introduction

Bimetallization is one of the useful approaches to improve catalytic activity because it induces changes in electronic and geometric structures of metal catalysts. For bimetallic systems, monolayer surfaces have been often studied [1]. Ag and Ni are known for being essentially immiscible due to differences of atomic sizes and cohesive energies [2]. Ag on Ni surfaces is expected to form an adlayer structure which shows strain effect. We have studied the adlayer structure of Ag on Ni(111) and CO adsorption on the adlayer.

II. Computational method

Spin-polarized DFT calculations were performed using the plane-wave pseudopotential approach in the PWscf code. GGA-PBE approximation was adopted. The energy cutoff of 30 Ry and Monkhorst-Pack mesh of 2×2×1 k-points were used. Surfaces were modeled using (4×4) or (5×5) unit cells consisting of four atomic layers.

III. Results and Discussion

To examine an adlayer structure of Ag/Ni(111), we calculated a two-dimensional (2D) island, a cluster and a dispersed layer of a Ag coverage of 0.25 ML using (4×4) unit cells. The 2D island was the most stable for the adlayer structure. We optimized CO adsorption on Ag/Ag(111) and Ag/Ni(111) with (5×5) unit cells as shown in Fig. 1. Table 1 shows the CO adsorption energies, the Bader charge of CO, and d-band center of the Ag adlayer (E_d). CO adsorption on Ag/Ni(111) was more stable by 0.17 eV than that on Ag/Ag(111), while E_d for Ag /Ni(111) nearly equals to that for Ag/Ag(111). Electron transfer to CO from Ag/Ni(111) is larger by 0.08e than that from Ag/Ag(111). This suggests that bimetallization of Ag and Ni enhance back donation from Ag atom to CO.

[1] Chen, J. G.; Menning, C. A.; Zellner, M. B. *Surf. Sci. Rep.* **2008**, *63*, 201.
[2] Li, Z.C.; Yu, D.P.; Liu, B.X. *Phys. Rev. B*, **2002**, *65*, 245403.

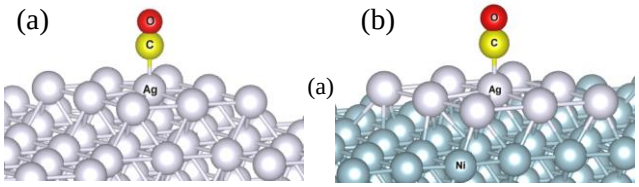

Table 1. CO adsorption energies, difference of the Bader charge of CO, and d-band center of Ag adlayer.

Surface	E_{CO} /eV	q	E_d /eV
Ag/Ag(111)	-0.14	-0.07	-3.93
Ag/Ni(111)	-0.31	-0.15	-3.95

PIIb-20

First-principles study of fast Na diffusion in Na_3P

Xuefang Yu, Giacomo Giorgi, Hiroshi Ushiyama, and Koichi Yamashita
Department of Chemica; System Engineering, School of Engineer, The University of Japan
Hongo, Bunkyo-ku, Tokyo 113-8656, Japan
e-mail address: xuefang@tcl.t.u-tokyo.ac.jp

I. Introduction

Elemental phosphorus is very appealing for the anode material of Na-ion battery, because it has high theoretical capacity of 2596 mA hg-1 when taking up three Na atoms to form the fully charged state (Na_3P) [1]. Ionic and electronic conductivity are the critical factors which determine the speed of charging and discharging process. In this work, first principle simulation was used to study the ionic conductivity and electron property in the fully charged state of P (Na_3P). The present work aims to theoretically estimate the electrochemical performance of P as anode in the first step of Na de-intercalation process.

II. Method

The density functional theory calculation was performed with VASP code. The electron-ion interaction and electron-electron interaction had been described by projector augmented waves pseudo-potentials and Perdew-Burke-Ernzerhof exchange and correlation functionals, respectively. Vacancy formation energies were calculated for the two kinds of Na vacancy. Nudged elastic band method was used to locate the saddle point and minimum energy paths for Na diffusion. Band structure calculation was performed to obtain the electronic properties.

III. Results and discussion

Three independent and asymmetric diffusion paths have been found as follows:

Path I: Na_{ax}@v → TS1 →Na_{ax}'@v , Path II: Na_{ax}@v → TS2 →Na_{ax}"@v

Path III: Na_{ax}@v → TS3 →Na_{eq}@v

Path I and Path II belongs to the Na diffusion taking place in the same kind of Na with small activation energy of 0.03 eV and 0.04 eV, respectively. While Na diffusion in Path III occurs within different kind of Na, and the energy barrier is estimated to be 0.26 eV. The lower energy barrier in Path I and Path II indicates the fast ionic conductivity in Na_3P.

Besides, with the introduction of Na vacancy, a hole state deep in the valence region appears, which is responsible for the valence band-edge raising in the center of the Brillouin zone. This sodium vacancy is very likely to play a role in the electron transfer in Na_3P. The fast ionic conductivity and considerable electronic conductivity make P as a promising anode material in the first step of Na de-intercalation process.

[1] H. Yang, et al., *Angew, Chem. Int. Ed.* 2013,**52**,1.

PIIb-21

The role of the inorganic cation MA ($CH_3NH_3^+$) in pseudocubic 3D $MAPbI_3$ organic-inorganic perovskites

Giacomo Giorgi[1,2], Jun-Ichi Fujisawa[1,3], Hiroshi Segawa[1], Koichi Yamashita[2]

[1]*Research Center for Advanced Science and Technology (RCAST), The University of Tokyo, 4-6-1, Komaba, Meguro-ku, 153-8904 Tokyo, Japan.*

[2]*Department of Chemical System Engineering, School of Engineering, The University of Tokyo,7-3-1, Hongo, Bunkyo-ku, Tokyo, Japan.*

[3]*Japan Science and Technology Agency (JST), Precursory Research for Embryonic Science and Technology (PRESTO), 4-1-8 Honcho Kawaguchi, Saitama 332-0012, Japan.*

e-mail address: giacomo@tcl.t.u-tokyo.ac.jp

Novel inorganic-organic hybrid systems have been suggested as potential alternatives in next generation dye-sensitized solar cells [1,2]. These composites are constituted by sandwiched structures of mesoporous TiO_2 and a "new-old" material, $CH_3NH_3PbX_3$ (X= Cl,Br,I) perovskites whose improved light harvesting quality is the driving force towards the achievement of high power conversion efficiency.

In our work, by means of a Density Functional based analysis [3], moving from a revise of the basic properties of the bulk perovskite, we focus on the inclusion of spin-orbit coupling effect in the band profile of such systems and on the role that the organic cation plays in the electronic properties of the final mixed system. We then report for the first time the theoretical prediction of the effective masses of the photocarriers, finding that effective masses of photogenerated electrons and holes are comparable to those for silicon used in commercially available inorganic solar cells

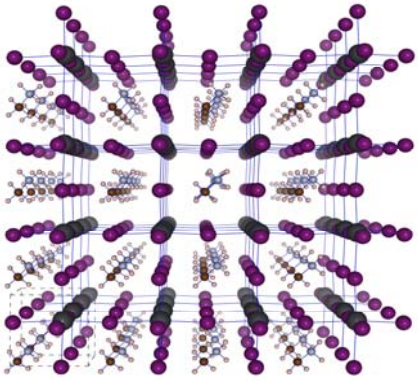

Fig. 1. Optimized structure of the cubic polymorph of $CH_3NH_3PbI_3$. [Large dark gray: lead,purple: iodine, brown: carbon, small light gray: nitrogen, white: hydrogen atoms]

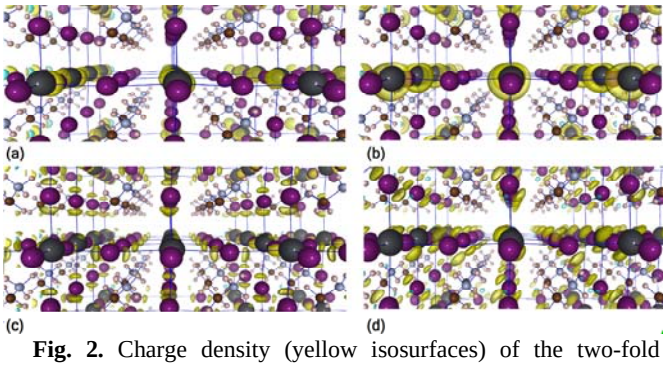

Fig. 2. Charge density (yellow isosurfaces) of the two-fold degenerate states ((a) and (b)) of the bottom of the conduction band and those ((c) and (d)) of the top of the valence band at *R* point calculated with spin-orbit coupling for (pseudo)-cubic $CH_3NH_3PbI_3$. [Large dark gray: lead,purple: iodine, brown: carbon, small light gray: nitrogen, white: hydrogen atoms].

[1] M. Liu *et al.* Nature 501, 395 (2013).[2] J. M. Heo *et al.* Nature Photonics 7, 486 (2013). [3] www.vasp.at

PIIb-22

DFT Probe on Electronic and Bonding Parameters of *n*NHC and *a*NHC Palladium Complex

N. Radhika[a], G.Velmurugan[b], P. Venuvanalingam[b] and M. Hada[a]
[a]*Department of Chemistry, Graduate School of Science and Engineering, Tokyo Metropolitan University, 1-1 Minami-Osawa, Hachi-Oji City, Tokyo, 192-0397, Japan*
[b]*School of Chemistry, Bharathidasan University, Tiruchirappallli 620024, Tamil Nadu, India*
e-mail address: radhika.narayanan.n@gmail.com

Metal coordinated abnormal N-heterocyclic carbene (*a*NHC) complexes have been found to be excellent catalysts in organometallic chemistry [1]. The abnormal mode of binding helps in strong binding to the metal due to its prominent σ-donating property. The *a*NHC is a strong electron donor ligand in metal complexes than its normal N-heterocyclic carbene (*n*NHC) isomer [2]. The *a*NHC complexes are efficient catalysts for various cross coupling reactions like Heck coupling and Suzuki-Miyaura coupling where *n*NHC is inactive under same conditions. Even though many palladium *a*NHC and *n*NHC complexes have been reported so far, their inherent properties have not been investigated thoroughly. The main focus of the work is the comparison of *n*NHC and *a*NHC palladium complexes in terms of bonding and electronic properties. DFT calculations were carried out in order to obtain insights into Pd-carbene bonding. FMO and NBO analysis were carried out to understand the nature of Pd-carbene bond and the relative activities of the *a*NHC and *n*NHC. The DFT calculations show that nucleophilic character at the carbene carbon in the *a*NHC ligand is higher than that of the *n*NHC. Further, Energy Decomposition Analysis (EDA) reveals that the palladium *a*NHC complexes possess high bonding interaction energy, compared to analogous *n*NHC complexes. Overall, these theoretical findings will give useful clues to develop new series of *a*NHC complexes that will act as better catalysts.

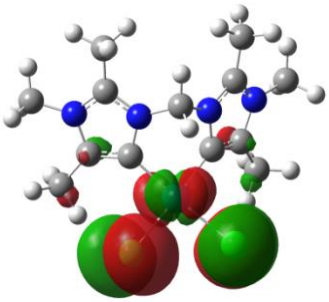

HOMO

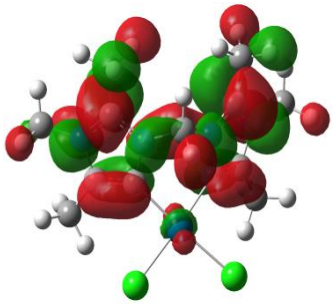

LUMO

References:
[1] Sau, S. C.; Santra, S.; Sen, T. K.; Mandal, S. K.; Koley, D. *Chem. Commun*. **2012**, *48*, 555.
[2] Aldeco-Perez, E.; Rosenthal, A. J.; Donnadieu, B.; Parameswaran, P.; Frenking, G.; Bertrand, G. *Science* **2009**, *326*, 556.

PIIb-23

Efficient geometry optimization using accurate two-component relativistic Hamiltonian with local unitary transformation scheme

Yuya Nakajima[1], Junji Seino[1], and Hiromi Nakai[1-4]

[1] *Department of Chemistry and Biochemistry, School of Advanced Science and Engineering, Waseda University, Tokyo 169-8555, Japan*

[2] *Research Institute for Science and Engineering, Waseda University, Tokyo 169-8555, Japan*

[3] *CREST, Japan Science and Technology Agency, 4-1-8 Honcho, Kawaguchi, Saitama 332-0012, Japan*

[4] *Elements Strategy Initiative for Catalysts and Batteries (ESICB), Kyoto University, Katsura, Kyoto 615-8520, Japan*

e-mail address: n-azure@ruri.waseda.jp

Relativistic effect is essential for reliable predictions of geometries for molecules including heavy-elements. In this study, we developed the analytical energy gradient of the one-particle infinite-order Douglas-Kroll-Hess (IODKH) [1] method combined with the local unitary transformation (LUT) scheme [2,3]. In the IODKH method, the Dirac Hamiltonian is completely block-diagonalized using one-particle unitary transformation. The unitary transformation in the LUT scheme is approximated as block-diagonal form of the subsystem contributions, which are adopted as atomic partitioning. Here using this partition simplifies the formulas of analytical derivatives of LUT-IODKH method as follows:

$$\frac{\partial}{\partial R_A}\left\langle \chi_\mu^A \middle| \mathbf{h}_2^{\mathrm{LUT}} \middle| \chi_\nu^B \right\rangle = \begin{cases} \dfrac{\partial}{\partial R_A}\left\langle \chi_\mu^A \middle| \sum_{C\neq A} \mathbf{V}_C^{\mathrm{NR}} \middle| \chi_\nu^B \right\rangle & (A=B) \\ \dfrac{\partial}{\partial R_A}\left\langle \chi_\mu^A \middle| \mathbf{V}_A^{+} + \mathbf{V}_B^{+} \middle| \chi_\nu^B \right\rangle + \dfrac{\partial}{\partial R_A}\left\langle \chi_\mu^A \middle| \mathbf{T}^{\mathrm{NR}} + \sum_{C\neq A,B} \mathbf{V}_C^{\mathrm{NR}} \middle| \chi_\nu^B \right\rangle & (A\neq B, R_{AB}\leq \tau). \\ \dfrac{\partial}{\partial R_A}\left\langle \chi_\mu^A \middle| \mathbf{T}^{\mathrm{NR}} + \sum_{C} \mathbf{V}_C^{\mathrm{NR}} \middle| \chi_\nu^B \right\rangle & (A\neq B, R_{AB}> \tau) \end{cases} \quad (1)$$

Here, A, B, and C are the subsystems, R_A is the coordinate of nucleus A, $\mathbf{T}^{\mathrm{NR}}$ is the kinetic operator, $\mathbf{V}^{\mathrm{NR}}$ is the nuclear-attraction operator, $\mathbf{V}^{+}$ is the relativistic nuclear-attraction operator, R_{AB} is the distance between atoms A and B, and τ is the threshold for cutoff of relativistic interaction, which is set to 3.5 Å. Figure 1 shows the system-size dependence of the CPU time in the IODKH or LUT-IODKH transformation of (a) one- and (b) three-dimensional silver clusters Ag_n. The results indicate that the LUT scheme drastically reduces the computational costs of conventional IODKH transformation. The scalings are liner even in three-dimensional clusters. In addition, numerical assessments of several molecular systems show that the obtained structures are good agreement with those of conventional IODKH and four-component relativistic scheme.[4]

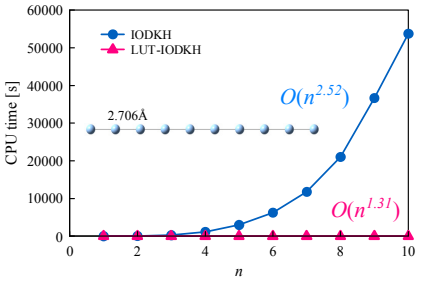

(a) One-dimensional silver cluster

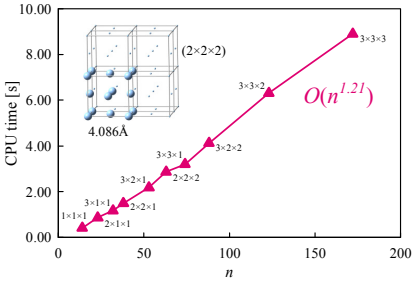

(b) Three-dimensional silver cluster

Fig. 1. System size dependence of CPU time

[1] M. Barysz and A. J. Sadlej, J. Chem. Phys. **116**, 2696 (2002). [2] J. Seino and H. Nakai, J. Chem. Phys. **136**, 244102 (2012). [3] J. Seino and H. Nakai, J. Chem. Phys. **137**, 144101 (2012). [4] Y. Nakajima, J. Seino, and H, Nakai, J. Chem. Phys. submitted.

PIIb-24

Diagonal Born-Oppenheimer Correction based on Relativistic Hamiltonians

Yuji Imafuku[1,2], Minori Abe[1,2], Michael.W.Schmidt[3], Terutaka Yoshizawa[1,2], Masahiko Hada[1,2]
[1]*Department of Chemistry, Graduate School of Science and Engineering, Tokyo Metropolitan University,1-1 Minami-Osawa, Hachi-Oji City, Tokyo, 192-0397, Japan,*
[2]*JST-CREST ,* [3]*Iowa State University*
e-mail address: Imafuku-yuji@ed.tmu.ac.jp

Electronic structure calculations in quantum chemistry are generally based on the Born-Oppenheimer approximation (BOA). The error generated by the BOA is negligibly small in most cases such as thermo-dynamical discussions in chemical reactions or molecular geometries. However, the BOA breaking effects are non-negligible in the sense of spectroscopic accuracy. Spectroscopic accuracy in experiments has been drastically improved during a few decades. The BOA breaking effects are possible to be observed in the current experimental techniques.

The first-order correction to the BOA in perturbation theory is so-called diagonal Born-Oppenheimer correction (DBOC). The DBOC is the expectation value of the nuclear kinetic-energy operators over the electronic wave function shown in Eq. (1).

$$\Delta E_{DBOC} = -\sum_{A}\sum_{i=x,y,z}\frac{1}{2M_A}\left\langle \Psi(\mathbf{r};\mathbf{R}) \middle| \nabla^2_{R_{Ai}} \middle| \Psi(\mathbf{r};\mathbf{R}) \right\rangle \quad . \qquad (1)$$

Here, the summation runs over all Cartesian coordinates R_{Ai} of a nucleus A in a molecule and *i* indicates *x*, *y*, and *z* components. M_A is the corresponding nuclear mass and $\Psi(\mathbf{r};\mathbf{R})$ is the normalized electronic wave function depending on the electronic coordinates **r** and nuclear coordinates **R**. The DBOC is studied by Handy *et al*. [1] in 1986 at the Hartree-Fock (HF) and multiconfiguration HF level. More recently, electron correlation is considered in a numerical CI level by Valeev and Sherril [2] and an analytical CC level by Gauss *et al*. [3]. However all of them are based on the non-relativistic Hamiltonian and discussions are limited in molecules composed by light atoms. Actually there is no knowledge that the BOA breaking effect is more or less significant in the systems with heavy atoms.

Hence in this study, we have developed a program to evaluate the DBOC based on relativistic Hamiltonians at the restricted HF level. We have adopted the 2nd-order and infinite-order Douglas-Kroll methods at their spin-free levels. In my poster, we will present how the DBOC terms change when molecular systems contain heavier atoms. We will also discuss the relativistic effect on the DBOC.

[1] N. C. Handy, Y. Yamaguchi, and H. F. Schaefer III, J. Chem. Phys. **84**. 4481 (1986)
[2] E. F. Valeev and C. D. Sherrill, J. Chem. Phys. **118**, 3921 (2003)
[3] J. Gauss, A. Tajti, M. Kállay, J. F. Stanton, and P. G. Szalay, J. Chem. Phys. **125**, 144111 (2006)

PIIb-25

Accuracy of the two-component methods in the relativistic molecular orbital theory

Nobuki Inoue, Satoshi Suzuki, Yoshihiro Watanabe, and Haruyuki Nakano
Department of Chemistry, Graduate School of Sciences, Kyushu University
6-10-1, Hakozaki, Higashi-ku, Fukuoka 812-8581, Japan
e-mail address: ion@ccl.scc.kyushu-u.ac.jp

I. Introduction

The two-component method in the relativistic electronic structure theory has now become a basic tool to treat the systems including heavy elements. It is cost-effective compared with the four-component method, and yet can yield very accurate results. However, the accuracy of various versions of two-component method have not been systematically examined so far. In the present study, we investigate the properties and accuracy of some widely-used versions of two-component method: the Breit–-Pauli approximation (BPA) [1], zeroth-order regular approximation (ZORA) [2], infinite-order regular approximation (IORA) [3], relativistic elimination of small component (RESC) [4], Douglas–Kroll (DK) [5], and infinite-order two-component (IOTC) [6] methods. New expressions of the DK2 and DK3 two-electron operators are also presented.

II. Computational methods

We carried out two-component calculations for (1) one-electron system using a single Gaussian basis function, (2) two-electron system using a single Gaussian basis function, and (3) helium-like ions using 45 Gaussian basis functions [7]. The programs for the two-component (BPA, ZORA, IORA, RESC, DK, and IOTC) methods including newly derived DK2 and DK3 two-electron operators, as well as the four-component (4-comp.) method, are implemented for the calculations.

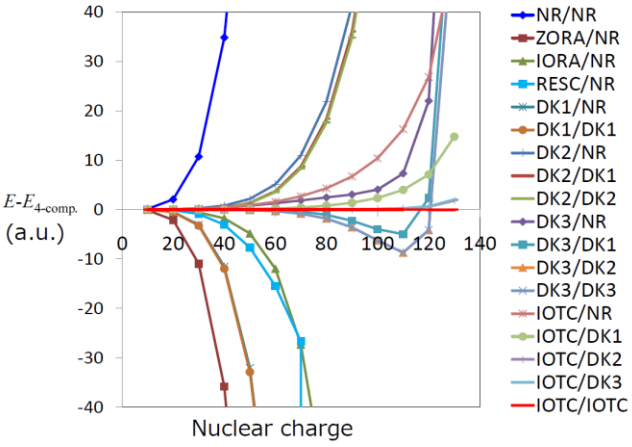

Fig. 1. Hartree–Fock energy of helium-like ions computed by various two-component methods. The energy values are measured from the energy by the four-component method. The symbol A/B means (one-electron term)/(two-electron term).

III. Results and discussion

The results for the one-electron system using a single Gaussian basis function showed that the accuracy of the total energy depends mainly on the accuracy of one-electron Hamiltonian and that the DK and IOTC one-electron Hamiltonians give quite accurate results.

Figure 1 shows the Hartree–Fock total energy of the helium-like ions computed by various two-component methods. The energies are so adjusted that the energy by the four-component method is to be the origin. Here the relativistic two-electron term is only considered by using the DK and IOTC methods. This figure clearly shows that IOTC/IOTC is extremely accurate. The energy line is almost on the four-component energy line. The figure also indicates that IOTC/DK2 and IOTC/DK3 are fairly good. The difference from the four-component line can be only seen for about Z > 110.

[1] H. A. Bethe and, E. E. Salpeter, *Quantum mechanics of one- and two-electron atoms*; Springer: Berlin, Heidelberg, New York, 1957. [2] E.van Lenthe, E.J.Baerends, and J.G.Snijders, J. Chem. Phys. **101**, 9783-9792 (1994) [3] K. G. Dyall and E. van Lenthe, J. Chem. Phys.**111**, 1366-1372 (1999) [4] T. Nakajima and K. Hirao. Chem. Phys. Lett.,**302**,383-391 (1999) [5] T. Nakajima and K. Hirao. Chem. Phys. Lett. **329** 511-516 (2000) [6] M. Barysz and A. J. Sadlej, J. Chem. Phys. **116**, 2696-2704 (2002) [7] J.Seino and M.Hada. Chem. Phys. Lett., **461**, 327-331 (2008)

PIIb-26

Time Evolution Simulation of Electronic Spin Based on Quantum Electrodynamics

Masahiro Fukuda, Kazuhide Ichikawa and Akitomo Tachibana
Department of Micro Engineering, Kyoto University,
Nishikyou-ku, Kyoto 615-8540, Japan
e-mail address: fukuda.masahiro.57w@st.kyoto-u.ac.jp

Recently, the development of nano technology and atom technology is remarkable and improved experimental tools enable us to treat even single photons and single electrons. Especially in the field of the spintronics, the electronic spin is one of the most interesting quantities for electronic devices and the further knowledge of the local effects of the electronic spin are required to control the spin more accurately. Despite the necessity, there are few theoretical studies for the local evolution of the electronic spin are reported. Therefore, the purpose of this study is simulating the electronic spin dynamics in a local region by first principle calculations.

The local dynamics of the electronic spin cannot be fully described in the framework of the quantum mechanics but the quantum field theory because of existence of local contribution, zeta force density [1, 2]. We assume the molecular system in a magnetic field and investigate a local picture of the electronic spin dynamics by the time evolution simulation based on the Rigged QED (Quantum ElectroDynamics) [1-4], which can treat the dynamics of electron, photon and nucleus in a quantum field theoretic way.

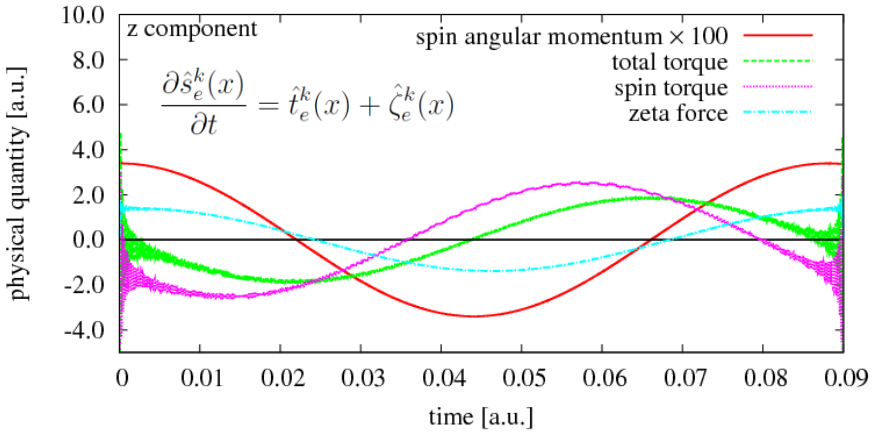

Fig.1 Time evolution of the local physical quantities at a point in a hydrogen atom.

[1] A. Tachibana, J. Mol. Struct. (THEOCHEM), **943**, 138 (2010).
[2] A. Tachibana, J. Math. Chem. 50, 669-688 (2012)
[3] *QEDynamics*, M. Senami, K. Ichikawa, A. Tachibana
http://www.tachibana.kues.kyoto-u.ac.jp/qed/index.html
[4] K. Ichikawa, M. Fukuda and A. Tachibana, Int. J. Quant. Chem. 113, 3, 190-202 (2013)

PIIb-27

Toward reliable prediction of hyperfine coupling constants using *ab initio* density matrix renormalization group method: diatomic π−radicals as test cases

Tran Nguyen Lan,[1] Yuki Kurashige,[1,2] ad Takeshi Yanai[1,2]

[1]*The Graduate University for Advanced Studies, Myodaiji, Okazaki, Aichi 444-8585, Japan*

[2]*Department of Theoretical and Computational Molecular Science, Institute for Molecular Science, Okazaki, Aichi 444-8585, Japan*

E-mail address: lantran@ims.ac.jp

Using the density matrix renormalization group (DMRG) method in conjunction with the complete active space (CAS) procedure, namely CAS configuration interaction (CASCI) and CAS self-consistent field (CASSCF), the hyperfine coupling constants (HFCCs) have been evaluated for a series of diatomic π−radicals. The electron correlation effects on the computed HFCC values were systematically investigated using various levels of active space, which were increasingly extended from the single valence space to the large-size model space entailing double valence and at least single polarization shells. In addition, the core correlation was treated by including the core orbitals in active space. It was found that the quite accurate results were obtained by the DMRG-CASSCF method involving orbital optimization, while DMRG-CASCI calculations with Hartree-Fock orbitals provided the HFCCs in poor agreements with experimental values. In order to get insights into the accuracy of HFCC calculations, we have analyzed the orbital contributions to the total spin density at the given nucleus, which is directly related to the FC term and numerically quite sensitive to the level of correlation treatments and basis sets. The convergence of calculated HFCCs with increasing number of renormalized states was also assessed. Our work serves as the first study on the performance of *ab initio* DMRG method for HFCC prediction.

Methods	^{27}Al				^{17}O			
	$A^{(K;c)}$	$A_{11}^{(K;d)}$	$A_{22}^{(K;d)}$	$A_{33}^{(K;d)}$	$A^{(K;c)}$	$A_{11}^{(K;d)}$	$A_{22}^{(K;d)}$	$A_{33}^{(K;d)}$
DMRG-CASCI(21e,36o)	710.91	−46.45	−46.62	93.06	1.82	44.98	44.89	−89.87
DMRG-CASSCF(21e,36o)	722.73	−54.19	−54.09	109.28	15.06	50.73	50.43	−101.16
B3LYP	512.21	−59.97	−59.97	119.93	8.17	66.22	66.22	−132.43
TPSS	656.79	−56.10	−56.10	112.21	9.52	59.91	59.91	−119.83
BP	653.71	−56.86	−56.86	113.72	14.21	59.60	59.60	−119.20
CCSD	482.40	−57.20	−57.20	114.30	18.10	63.80	63.80	−127.70
CCSD(T)	565.30	−56.20	−56.20	112.40	19.30	58.90	58.90	−117.80
Exp – gas-phase	738	−56	−56	112	n/a			
Exp – Ne-matrix	766	−52	−52	104	2	50	50	−100

Table.1 HFCCs (in MHz) for AlO radical. The IGLO-III and EPR-III basis sets were used for Al and O, respectively. The total number of AOs is of 84.

PIIb-28

A New Diagrammatic Interpretation of Fitzgerald-Lorentz Contraction in Special Relativity

Shigeru Obara
Department of Chemistry, Kushiro Campus, Hokkaido University of Education
Shiroyama 1-15-55, Kushiro 085-8580, Japan
e-mail address: obara.shigeru[at]k.hokkyodai.ac.jp

I. Introduction

Introducing various ways of representing the laws of physics is expected to lead students to a better understanding of nature, and Fitzgerald-Lorentz contraction in special relativity is one such scientific consideration. This contraction is given from a purely logical way of thinking based on assumptions such as the laws of physics being identical in all inertial frames. As it is purely logical, students sometimes find it hard to visualize its meaning. Accordingly, in the present paper we give a diagrammatic interpretation of the contraction based on the well-known diagram obtained from the Michelson-Morley experiment. This interpretation is the first of its kind as far as the author knows. Also outlined is a simple method of depicting the contracted length on a diagram based on the interpretation, and proof is given using both geometrical and analytical methods.

II.Discussion

A schematic diagram of the Michelson-Morley experiment is shown in **Fig. 1**. A light source is placed at *O* and two mirrors at *H* and *V*. The distance from *O* and the mirrors is the same so the light signals emitted simultaneously at the origin *O* will return to *O* simultaneously. When the apparatus is moving horizontally, two light signals travel in the "vertical" and horizontal directions as shown in **Fig. 2**. The moment the horizontal light signal arrives at *A*, the vertical light signal arrives at a point *D* the same distance (*AO′* = *DO′*) away from *O′*. The light source should therefore be at *O″*, since it is always right below the vertical light signal. Therefore the contracted horizontal length results in *AO″* (red line), while the original length is *BC* (blue line). Note that the length of the red line is the same as a sum *DO′*+*O′O″* of two sides of the rectangular triangle ∆*DO′O″*. The contracted length can be depicted easily on the Michelson-Morley diagram by drawing a line orthogonal to the segment *BO′* from *C* (**Fig. 3**). The crossing point denoting as *E*, the segment *BE* has the contracted length. A geometric proof of the contracted length is as follows: The triangle ∆*BFG* being set to be congruent with the triangle ∆*DO′O″* in **Fig. 2**, two red line segments *FO′* and *CO′* have the same length (note that *AO′*+*CO′*=*BO′* in Fig.2) and the line segments *CO′* and *GF* being parallel, two angles denoted by red crosses (“x”) are proved to be the same, so that the triangles ∆*FGC* and ∆*FEC* become congruent. Then we obtain the relation *FG* = *FE*, and finally get *BE* = *AO″*, which is the contracted length. The contracted length becomes shorter as the speed increases (**Fig. 4**) since the triangle becomes flatter, and the crossing point *E* becomes nearer to *B*. The point *E* is actually a point on a semicircle with a diameter of *BC*.

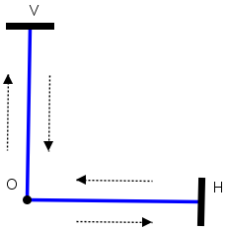

Fig. 1. Schematic diagram of the Michelson-Morley experiment.

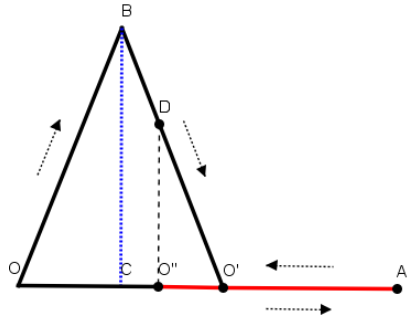

Fig. 2. Paths of light signals traveling in the "vertical" and horizontal directions in the Michelson-Morley experiment with horizontally moving apparatus.

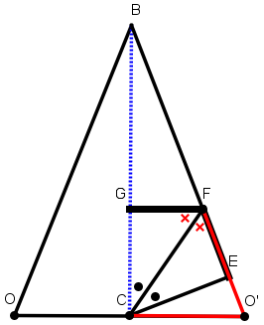

Fig. 3. The contracted length on the diagram.

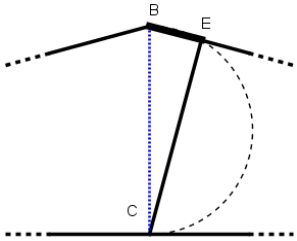

Fig. 4. The contracted length becomes shorter as the speed increases.

PIIb-29

Efficient antisymmetrization theory for accurate molecular wave functions: *i*Exg theory

Hiroshi Nakatsuji and Hiroyuki Nakashima
Quantum Chemistry Research Institute,
Katsura, Nishikyou-ku, Kyoto 615-8510, Japan
e-mail address: h.nakatsuji@qcri.or.jp

The governing principle of chemistry is the Schrödinger equation (SE) in which the wave function is determined with the Hamiltonian of the system under the constraint of the Pauli principle that requires antisymmetry for the exchange of any two electrons. Our aim is to establish a useful general method of solving the SE of many-electron atoms and molecules. Therefore, the efficient method of solving the SE and the efficient method of making the wave function antisymmetric are both the central subjects in our research. Such method would enable us to predict and even to simulate complex chemistry quite accurately.

The method of solving the SE was given by the present author [*See a review, Acc. Chem. Res.* 45, 1480 (2012)]. I use here the *free complement (FC) method.* We use the VB type formulation because first the Coulomb potential in the Hamiltonian is local and second we do not want to import the famous fault of the MO method in describing the potential curve of the homogeneous bond fission.

In actual calculations of the FC-LSE (local SE) method applied to many electron atoms and molecules, the antisymmetrization step is most time consuming, so that finding an efficient antisymmetrization method is crucially important. Now, we have two efficient anti-symmetrization methods, the Nk method [*J. Chem. Phys.* 139, 044112 (2013)] and the iExg method [to be published]. The former is a determinant-based method that is proportional to $N^{3\text{-}4}$ in average in many FC-LSE calculations. In the latter iExg (inter Exchange) theory, we perform antisymmetrizations after classifying them into atomic and interatomic ones. For example, for diatomic molecule AB, the antisymmetrizer A_{AB} is written as

$$\mathsf{A}_{AB} = \mathsf{A}_A \mathsf{A}_B (1 + E_{AB}^{(1)} + E_{AB}^{(2)} + \cdots + E_{AB}^{(i)} + \cdots + E_{AB}^{(K)})$$

where A_A is the antisymmetrizer for the electrons belonging to atom A and $E_{AB}^{(i)}$ is the *i*-electron exchange operator between A and B and *K* is the lesser of the numbers of electrons belonging to A and B. It is shown that the exchange contribution decreases exponentially as the number of the exchange increases and as the AB distance increases. Therefore, for large molecules, the number of exchanges necessary for antisymmetrization decreases dramatically, which leads the calculations to order-N type.

We will apply the above methodology of solving the SE to several different systems including organic molecules.

PIIb-30

Determinant-based antisymmetrization theory for the partially correlated wave functions: Nk algorithm

Hiroyuki Nakashima and Hiroshi Nakatsuji
Quantum Chemistry Research Institute,Katsura, Nishikyou-ku, Kyoto 615-8510, Japan
e-mail address: h.nakashima@qcri.or.jp

We proposed a fast antisymmetrization procedure, referred to as Nk algorithm [1], for the partially correlated wave functions that appear in the free complement-local Schrödinger equation (FC-LSE) method [2,3].

Pre-analysis of the correlation diagram, referred to as dot analysis, combined with the determinant update technique based on the Laplace expansion, drastically reduces the orders of the antisymmetrization computations. In the dot analysis, we first analyze the correlation diagram for the inseparable two-electron terms, such as $f_{ij}(i,j) = r_{ij}$, $r_{ij}^{\,2}$, $\exp(-\alpha r_{ij})$, and this process can minimize the number of electrons (dot electrons) that must be put outside of the determinant. Figure 1 shows the correlation diagrams and the circle points describe the dot electrons. This pre-analysis is based on the fact that the electronic Hamiltonian and its exact FC wave function of the SE are composed of only one- and two-body inseparable terms. By combining the determinant update method, the computational cost could be further reduced. Table I summarize the calculation orders for several different types of the partially correlated wave functions that appear in the FC wave functions within order 4. When the functions include only up to single-correlated terms, the order of computations is $O(N^3)$, which is the same as the non-correlated case. The worst calculation order is $O(N^6)$ but the number of these terms is quite limited. As a result, in many cases, the averaged calculation order becomes $O(N^3$-$N^4)$. However, this method is not very suitable for complex wave functions. A new alternative antisymmetrization theory, called *i*Exg algorithm, was also proposed by Nakatsuji and it is presented in the former poster.

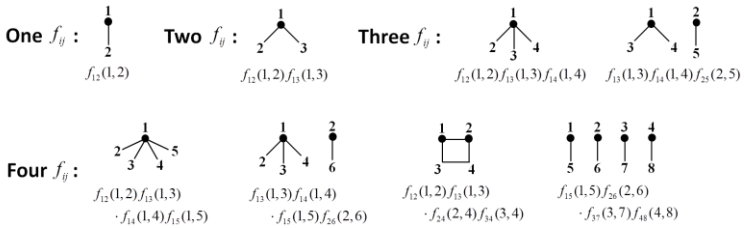

Fig. 1. Correlation diagrams for each type of the correlated function

Table I. The calculation orders of the Nk-algorithm for each type of correlated function

Correlated functions	Calculation order
No correlated function:	$O(N^3)$
One f_{ii} :	
$f_{12}(1,2)$	$O(N^3)$
Two f_{ii} :	
$f_{12}(1,2)\, f_{13}(1,3)$	$O(N^3)$
Three f_{ii} :	
$f_{12}(1,2)\, f_{13}(1,3)\, f_{14}(1,4)$	$O(N^3)$
$f_{13}(1,3)\, f_{14}(1,4)\, f_{25}(2,5)$	$O(N^4)$
Four f_{ii} :	
$f_{12}(1,2)\, f_{13}(1,3)\, f_{14}(1,4)\, f_{15}(1,5)$	$O(N^3)$
$f_{13}(1,3)\, f_{14}(1,4)\, f_{15}(1,5)\, f_{26}(2,6)$	$O(N^4)$
$f_{12}(1,2)\, f_{13}(1,3)\, f_{24}(2,4)\, f_{34}(3,4)$	$O(N^5)$
$f_{15}(1,5)\, f_{26}(2,6)\, f_{37}(3,7)\, f_{48}(4,8)$	$O(N^6)$

We have applied the present method to small atoms and molecules. We continue to develop the methods and computational algorithms to be more easily applicable to more general atoms and molecules.

[1] H. Nakashima and H. Nakatsuji, *J. Chem. Phys.* **139**, 044112 (2013). [2] H. Nakatsuji, *J. Chem. Phys.* **113**, 2949 (2000). H. Nakatsuji, *Phys. Rev. Lett.* **93**, 030403 (2004). H. Nakatsuji, *Phys. Rev. A* **72**, 062110 (2005). H. Nakatsuji, H. Nakashima, Y. Kurokawa, and A. Ishikawa, *Phys. Rev. Lett.* **99**, 240402 (2007). [3] H. Nakatsuji, *Acc. Chem. Res.* **45**, 1480 (2012). H. Nakatsuji, *Simulation*, **32**, 39 (2013).